Structural, Optical and Ellipsometric Characteristics of Synthesized SnO_2 Nanoparticles on Pt Coated Silicon Wafers

H. HOWARI[1] and I.B.I. TOMSAH[2]

a Physics Department, Deanship of Educational Services, Qassim University,
b Physics Department, College of Science, Qassim University, P.O. 6644, 51452
Buraidah, Kingdom of Saudi Arabia, Corresponding author: haidarh1@yahoo.com

Abstract:

Tin oxide nanoparticles were prepared on Pt-Si wafers by physical vapor deposition technique. The development of rutile structure of SnO_2 was revealed by XRD measurements after annealing the thin films at 750 ^{0}C for two hrs. The formation of tetrahedral shape nanoparticles at different size distributed randomly on the Pt-Si wafer was confirmed by SEM images. The refractive index, extinction coefficient, thickness, and roughness of the thin films were estimated using ellipsometric measurements. The energy bandgap of the SnO_2 thin films was calculated from the spectrophotometric measurement and is found to be 3.6±0.02 eV before and 3.8±0.02 eV after annealing, respectively.

Keywords: Ellipsometer, Nanoparticles, Refractive index, X-ray diffraction, Optical properties, F. Annealing

Introduction

The wide variety of electrical and optical properties of metal oxides makes them exciting materials for basic research and technological applications alike. Metal oxides span a wide range of electrical and optical properties from wide band gap insulators and lasers to metallic, superconducting and field emitting materials. Tin Oxide (SnO_2) has attracted considerable interest over many years owing to its huge range of applications. SnO_2, as an oxygen defect n-type transparent conducting material, which displays high infrared reflectance in addition to high visible light transmittance (80-90%) due to the wide band gap (Eg > 3 eV)[1-6]. SnO_2 is also having low electrical resistance [7]. It has been widely applied as heat mirrors, transparent conductive electrodes for solar cells, optoelectronic devices, and gas sensing material for gas sensors devices, catalyst supports, and solar cells [1-8]. Tin oxide films is the most used material because of its inexpensive raw material and highly existing in nature. It is characterized by a wide band gap and high electrical conductivity due the existing of O_2 vacancies and interstitial tin atoms in the crystal structure of the films which depends on the method of preparation. Also it is a good transparent anti-reflecting material. So far, attention has focused on the utilizations of a SnO_2 transparent electrode to electronic devices for example electrochromic, electroluminescent and gas sensing [7,8]. At present, different methods can be applied to prepare tin oxide films on several different substrates. The synthetic methods for SnO_2 nanostructures include laser ablation, reactive RF sputtering; dip deposition, chemical vapor deposition (CVD), spray pyrolysis, electro deposition, thermal oxidation, sol-gel dip coating, dc magnetron and thermal evaporation [7-9]. Among these, thermal evaporation method is a straight forward and does not require sophisticated instruments such as high vacuum systems. Moreover, thermal evaporation is the most popular way for nanostructures because of it easiness, low cost and readily available and the parameters are simply controlled. SnO_2 films can be deposited on different substrate materials such as glass, stainless steel, aluminum, silicon, Al_2O_3 and niobium. There are some

literatures reported the preparation of SnO_2 films using thermal evaporation methods [10]. Temperature stability and reproducibility of the film properties are important for device reliability. The exposure to heat after the preparation of the thin films may cause structural changes which tend to either influence or degradation in most of the physical properties of the films.

The aim of this work is to present a structural, morphological and optical study of SnO_2 thin films deposited on silicon wafers using physical vapor deposition technique (PVD). Also, the effects of annealing in air on structural and optical properties of SnO_2 thin films are studied. First, experimental details of the film will be given. Then, the structure and morphology of the films will be studied using x-ray diffraction measurements (XRD) and scanning electron microscope (ESM), respectively. The refractive index, absorption coefficient, optical gap energy and film thickness, will be calculated from the spectroscopic ellipsometry. Finally, a comparison of these results with those of other works will be given.

Experimental

The SnO_2 nanoparticles thin films were grown using physical vapor deposition technique. The growth method of tin oxide nanoparticles is based on thermal evaporation of Tin (IV) Oxide powder (Sigma-Aldrich chemicals 99.99%) with the presence of Pt catalyst. The synthesis was carried out on Pt coated (~10–15 nm) Si (100) wafers (cut into 1x1 cm^2 and ultrasonically cleaned). The preparation was carried out using Edwards PVD System. The samples were then annealed in air using furnace at 750 ^{0}C for about 2 hrs. The surface morphology and crystal structure of the synthesized nanoparticles thin films were characterized by scanning electron microscope (SEM) type JOEL model JSM-6380 LA (Japan) and X-ray diffraction (XRD) using Shimadzu Diffractometer XRD 6000, Japan, which utilizing $CuK_{\alpha 1}$ radiation (λ=1.54056 A˚), respectively. The crystal structure investigation data was performed by step-scan modes, in a 2θ range between 10^0 and 80^0 with step- size 0.02^0 and step time of $0.6s$. The spectroscopic ellipsometry (SE) data for SnO_2 thin films were acquired using a J.A.Woollam variable angle spectroscopic ellipsometer (J.A.Woollam corporation), in the wavelength range 400–1800 nm. The data was acquired at angle of incidences of 70^0 and 75^0. The measurements were conducted at room temperature. The instrument measures the complex ratio of the Fresnel reflection coefficients for p- and s-polarized light and reports the ratio in terms of the ellipsometric parameters Ψ and Δ defined by the equation:

$$\tilde{\rho} = \frac{\tilde{r}_p}{\tilde{r}_s} = \tan\Psi \exp(i\,\Delta) \qquad (1)$$

where $\tilde{r}_p$ and $\tilde{r}_s$ are the amplitude reflection coefficient for light polarized in the p- and s- plane of incidence, respectively. Ellipsometry does not directly measure the optical properties and thickness of a thin film; however, $\tilde{r}_p$ and $\tilde{r}_s$ are functions of these characteristics, which require data analysis for extraction. The starting point for such analysis is an optical model for the sample.

The data obtained from the ellipsometer were accurately modeled using the J.A.Woollam corporation developed WVAS32 software package. Ellipsometric data Ψ and Δ for variable wavelengths were fitted in the optical model. The transmittance measurements were carried out using a double-beam (Jasco UV-Vis-NIR-570 combined with PC) computer- controlled spectrophotometer, at normal incidence of light and in a wavelength between 200 and 2500nm.

Results and Discussion

Structural properties of thin films

The effect of annealing temperature on the characteristics properties of nanoparticles have been investigated over many years. Usually, increasing the annealing temperature, leads to structural changes from amorphous to crystalline and grain growth occurs. The XRD patterns of the deposited films before and after the annealing process are shown in Fig. 1. The samples were annealed in air at 750 ^{0}C for 2 hrs. No peaks are detected from the grown sample which confirms the amorphous nature of this sample. Annealing the sample at 750 ^{0}C shows relatively high peaks indicating the evolution of the polycrystalline behavior. The presence of platinum in the sample structure appears to induce a little change in the texture of the film. From the indexed diffraction peaks (110), (101), (200), (220), (210) and (301), the rutile structure of SnO_2-Pt with lattice constants a= 4.738 A˚, and c= 3.187 A˚ was confirmed (JCPDS file no. 41-1445). The annealed sample shows high intensity for (200) and (110) planes.

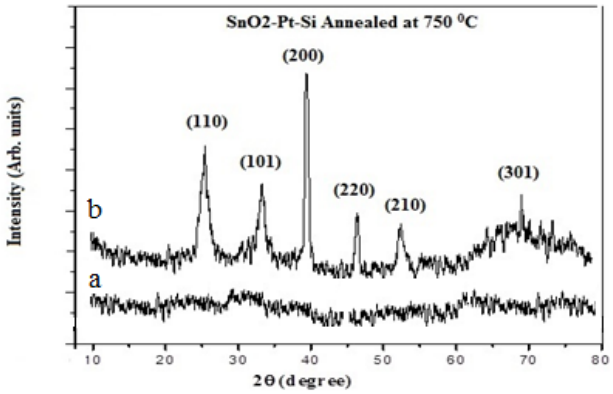

Fig.1. X-ray diffraction pattern of the synthesized SnO_2 nanoparticles thin film before (a) and after (b) the annealing process

This is due to the tendency for texturing towards (200) and (110) planes. Reports of increase in crystallinity with different annealing temperatures can be seen in literature [5].

Surface morphology of thin films

Regarding Scanning Electron Microscopy (SEM) characterization, all samples show the presence of a granular structured film of SnO_2 with randomly distributed shaped nanoparticles on the surface. Typical SEM images presenting morphologies of the synthesized SnO_2 on Pt coated Si wafers are shown in Fig. 2a and b, with lower and higher magnifications, respectively. It is shown that the white SnO_2 products are nanoparticles with different size. The top features are clearly tetrahedral shape. The particles are distributed randomly on the Pt coated Si wafers. The average particle size obtained from SEM images is in the range of 50 nm to 100 nm. It is found that the SnO_2 films have relatively smooth morphology [3].

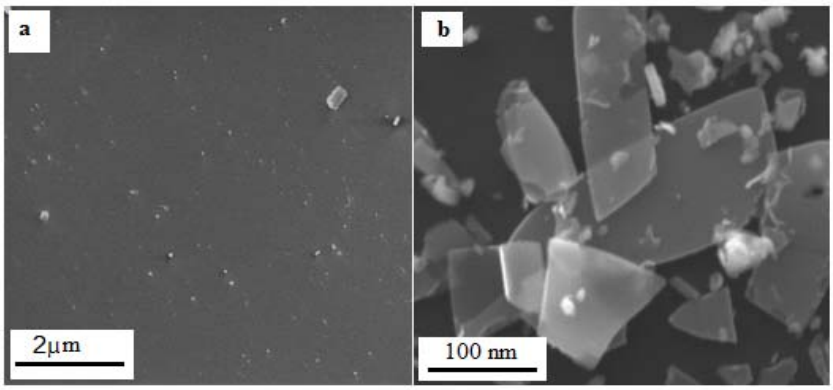

Fig.2. SEM images of the synthesized SnO_2 thin films at low (a) and high magnification (b).

Ellipsometric modulation

The choice of the appropriate optical model plays a major role in the evaluation of the optical constants from the SE spectra. Thus, the thickness of the SnO_2 thin films, refractive index (n), extinction coefficient and roughness were obtained by assuming a model: Si with absorbing film. An example for the best fit of the proposed model compared with the measured ellipsometric data of SnO_2 films at 70^0 and 75^0 angles of incidences for both Delta Δ and Psi Ψ is shown in Figures 3, 4, 5, and 6, before and after the annealing process. Clearly, there is good agreement between the simulated and the measured data over the entire measured wavelength range. Thus the optical constants can be adequately extracted. Table 1 summarizes some of these constants.

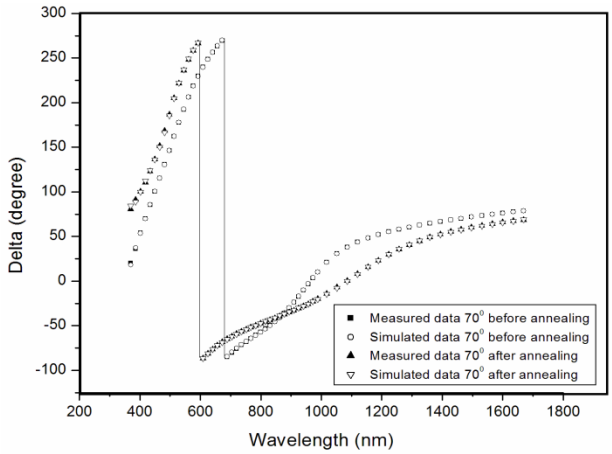

Fig.3. Measured and simulated Δ spectra at angle of incidence 70^0 of the SnO_2 nanoparticles thin films before and after the annealing process.

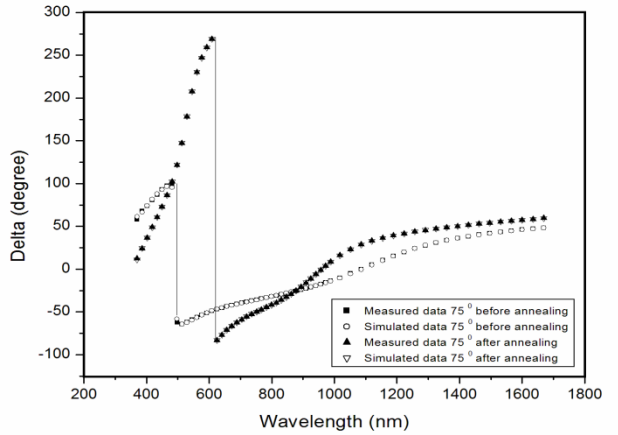

Fig.4. Measured and simulated Δ spectra at angle of incidence 75^0 of the SnO_2 nanoparticles thin films before and after the annealing process.

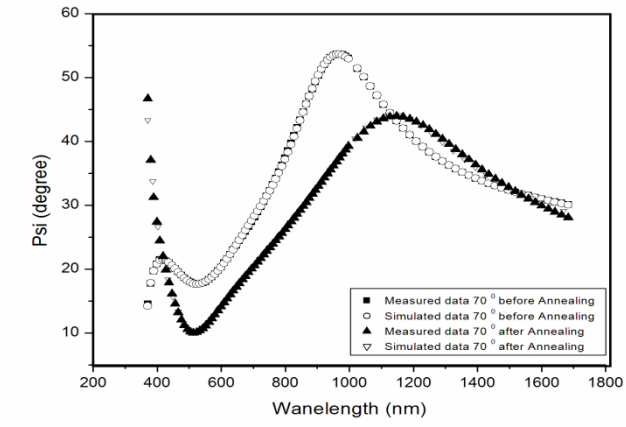

Fig.5. Measured and simulated Ψ spectra at angle of incidence 70^0 of the SnO_2 nanoparticles thin films before and after the annealing process.

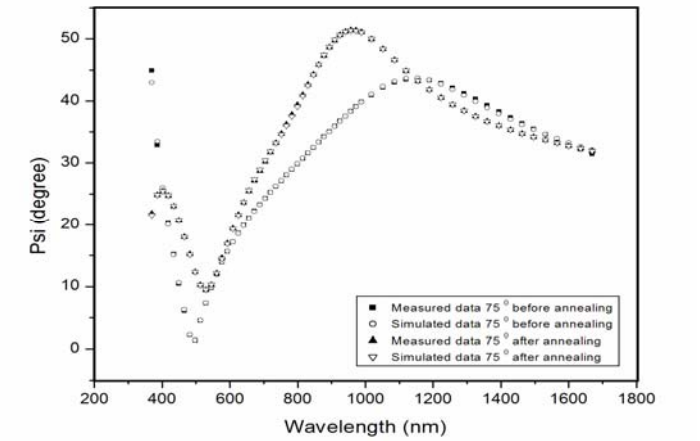

Fig.6. Measured and simulated Ψ spectra at angle of incidence 75^0 of the SnO_2 nanoparticles thin films before and after the annealing process.

The measured and simulated refractive index and extinction coefficient spectra of the SnO_2 nanoparticles are shown in Figures 7, and 8 and in good agreement with reported data [11].

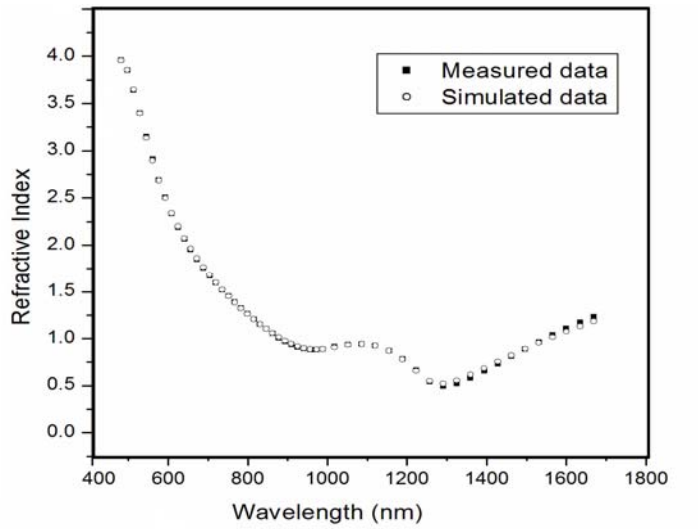

Fig.7. Measured and simulated refractive index (n) of the SnO_2 nanoparticles thin films.

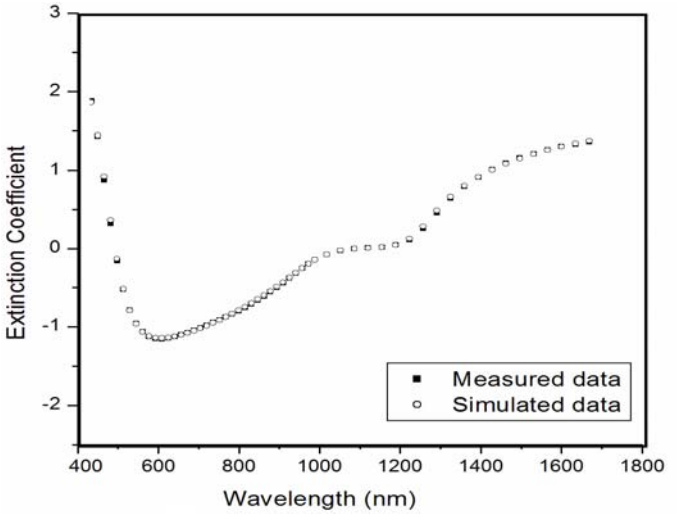

Fig.8. Measured and simulated extinction coefficient (k) of the SnO_2 nanoparticles thin films.

Table.1. Refractive index, extinction coefficient, thickness, and roughness of the SnO_2 nanoparticles thin films calculated by the ellipsometric measurements

	Before Annealing	After Annealing
Refractive index	2.388	2.115
Extinction coefficient	0.209	0.151
Thickness	110.16 ± 1.636 nm	135.99±2.301
Roughness	8.01 ± 1.095 nm	19.87±1.093
MSE	2.972	5.875

Optical Properties

Fig.9 shows the reflectivity spectra of the SnO_2 thin films before and after the annealing process. The presence of Pt particles is confirmed by the peak at 560 nm in the reflection spectrum, which is in consistence with the literature [12]. It seems that annealing the samples at 750 ^{0}C creates a blue shift of the absorption edge into higher energy.

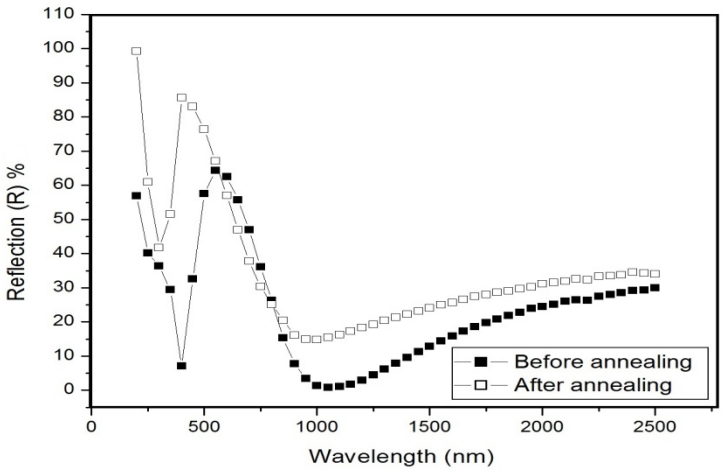

Fig.9. Reflectivity spectra of the synthesized SnO_2 nanoparticles thin films before and after annealing at 750 ^{0}C.

Fig.10 shows the absorbance spectra of the SnO_2 thin films before and after the annealing process. It displays a shift into higher energies after annealing, also the intensity decreases by a small fraction.

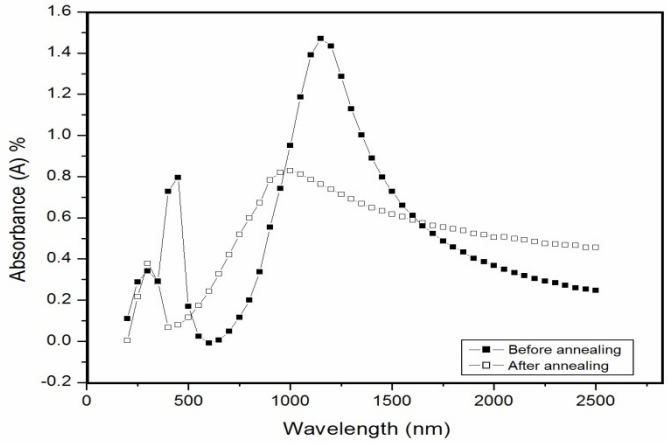

Fig.10. Absorbance spectra of the synthesized SnO_2 nanoparticles thin films before and after annealing at 750 ^{0}C.

The absorption coefficient (α) was calculated using the obtained k values from the relation:

$$\alpha = \frac{4\pi k}{\lambda} \tag{2}$$

The optical transitions of SnO_2 semiconductor have been shown to be a direct transition. The variation in the absorption coefficient α as a function of photon energy for direct transitions is given by [13]:

$$(\alpha h\nu) = (h\nu - E_g)^{1/2} \tag{3}$$

where A is a constant, h is Planck's constant, ν is the frequency, and E_g is the band gap energy. The direct band gap values are obtained by extrapolating the linear part to intercept with the energy axis and are

found to be 3.6±0.02 eV and 3.8±0.02 eV (Fig. 11), before and after annealing respectively. However, the E_g value appears to be in reasonable agreement with previous results reported for SnO_2 [3,5].

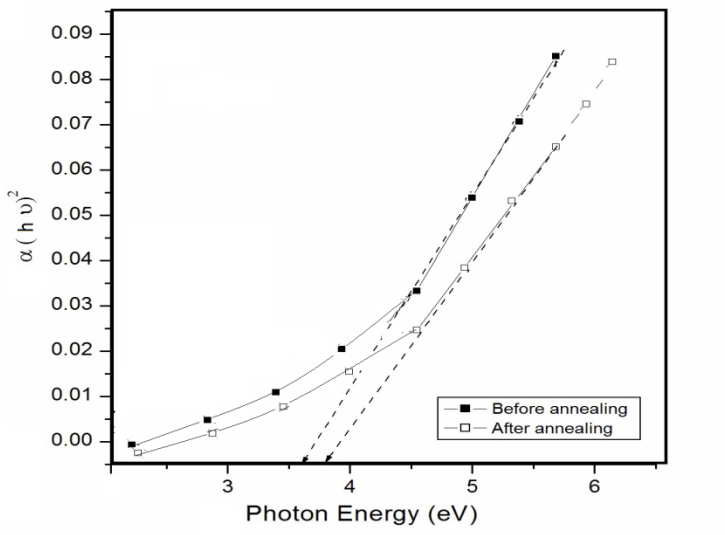

Fig.11. Plot of $(\alpha h\nu)^2$ vs photon energy ($h\nu$) before and after annealing at 750 ^{0}C.

Conclusion

The preparation of SnO_2 nanoparticles thin films on Pt-Si wafers is achieved by physical vapor deposition method. The XRD of the samples revealed the formation of rutile structure of SnO_2 after furnace annealing at 750 ^{0}C for two hrs. The SEM images confirm the formation of with tetrahedral shape nanoparticles at different size distributed randomly on the Pt-Si wafer. The refractive index, extinction coefficient, thickness, and roughness of the thin films were obtained using ellipsometric measurements. The energy bandgap of the SnO_2 thin films is found to be 3.6±0.02 eV before and 3.8±0.02 eV after annealing, respectively. The E_g value appears to be in reasonable agreement with previous results reported for SnO_2.

Acknowledgment

This work is supported by SABIC Company & Deanship of Scientific research at Qassim University, Saudi Arabia under contract No. SR-S-14-26. The authors thank Dr. M. GASSOUMI for his technical support and useful discussion.

References

[1]. N.M. Shaalan, T. Yamazaki, T. Kikuta, Mater. Chem. Phys. 127 (2011) 143.
[2]. B.-G. Kim, D.-G. Lim, J.-H. Park, Y.-J. Choi, J.-G. Park, Appl. Surf. Sci. 257 (2011) 4715.
[3]. GANESH E PATIL, D D KAJALE, D N CHAVAN, N K PAWAR, P T AHIRE, S D SHINDE, V B GAIKWAD and G H JAIN, Indian Academy of Sciences. Bull. Mater. Sci., Vol. 34, No. 1, February 2011, pp. 1–9.
[4]. S.H. Mohamed, Journal of Alloys and Compounds 510 (2012) 119– 124
[5]. Pawan Chetri, Amarjyoti Choudhury, Physica E 47 (2013) 257–263.

[6]. I.S. Hwang, S.J. Kim, J.K. Choi, J. Choi, H. Ji, G.T. Kim, G. Cao, J.H. Lee, Sens. Actuators B 148 (2010) 595.
[7]. M. Batzill and U Diebold, Progress in Surface Science 79 (2005) 47-154.
[8]. In-Sung Hwang, Young-Jin Choi, Jae-Hwan Park, and Jae-Gwan Park, Journal of the Korean Physical Society, Vol. 49, No. 3, September 2006, pp. 1229-1233
[9]. L.S. Chuah, International Journal of Advanced Technology in Engineering and Science Volume No.03, Issue No. 01, January 2015.
[10]. N. Kakati, J. Maiti, S.H. Jee, S.H. Lee, Y.S. Yoon, J. Alloys Compd. 509 (2011) 5617.
[11]. N F Habubi, K A Mishjil and S. S. Chiad, Indian J Phys (March 2013) 87(3):235–239.
[12]. C.Zhao, S. Qu, Q,Zaho, J. Qiu, C. Zhu, J. Sol-Gel Sci. Technol. 37 (2006) 5.
[13]. J. Robertson, J. Phys. Chem, 12 (1979) 4767.